

Femtosecond Time Resolved Fluorescence Dynamics of a Cationic Water-Soluble Poly(fluorenevinylene-*co*-phenylenevinylene)

Mihalis Fakis,* Dimitris Anestopoulos, Vassilis Giannetas, and Peter Persephonis

Department of Physics, University of Patras, Patras 26500, Greece

John Mikroyannidis

Department of Chemistry, University of Patras, Patras 26500, Greece

Received: November 4, 2005; In Final Form: May 12, 2006

A recently synthesized cationic water-soluble poly(fluorenevinylene-*co*-phenylenevinylene) was studied by means of steady state and femtosecond time resolved upconversion spectroscopy in aqueous and EtOH solutions. Steady state spectroscopic measurements showed that the polymer emits at the blue-green spectral region and that aggregates are formed in concentrated polymer solutions. The fluorescence dynamics of the polymer in concentrated solutions, studied at a range of emission wavelengths, exhibited a wavelength dependent and multiexponential decay, indicating the existence of various decay mechanisms. Specifically, a rapid decay at short emission wavelengths and a slow rise at long wavelengths were observed. Both features reveal an energy transfer process from isolated to aggregated chains. The contribution of the energy transfer process as well as of the isolated chains and the aggregates on the overall fluorescence decay of the polymer was determined. The dependence of the energy transfer rate and efficiency on polymer concentration was also examined.

Introduction

Conjugated polymers constitute a well-known class of materials for applications in optoelectronics and microelectronics such as lasers,¹ light emitting diodes,² photovoltaic cells,³ and transistors.⁴ The research realized on conjugated polymers during the last 15 years has been motivated by their remarkable photonic and electronic properties as well as low cost preparation. This research has led to major progress in the performance of polymeric devices reaching industrial standards.

Recently, water-soluble conjugated polymers (WSCPs) have been synthesized,^{5–10} and their successful preparation constitutes the most important step toward new envisioned applications in biology. Water solubility is offered through the addition of charged groups in the polymer's side chains so that conjugated polyelectrolytes are formed. Apart from water solubility, these polymers have a high absorption cross section in the UV–visible, high photoluminescence (PL) efficiency in the visible spectrum, excellent film forming properties, and inexpensive preparation.

Water-soluble polymers based on poly(*p*-phenylene) (PPP),¹¹ poly(*p*-phenylenevinylene) (PPV),¹² and polyfluorene (PFO)¹³ have been studied in the past. Both anionic and cationic conjugated polymers have been synthesized and examined as biological sensors.^{14,15} However, after the report by Gaylord et al.¹⁵ that a cationic PFO derivative could be used for real time detection of DNA, cationic polymers attract greater attention. In polymeric biosensors, the main photophysical phenomenon is excitation energy transfer from the water-soluble polymer to a dye related with the presence of the target biomolecule. This energy transfer causes quenching of the polymer's fluorescence.

Excitation energy transfer in conjugated polymers has been studied in the past and has been identified either as interchain or as intrachain (exciton migration).^{16–19} According to the Förster theory,²⁰ the spectral overlap between the donor's emission spectrum and the acceptor's absorption spectrum plays a crucial role in energy transfer. However, Tan et al. have recently reported that energy transfer from a conjugated polyelectrolyte to a charged dye (i.e., quenching of the polymer) does not always follow the Förster theory but is controlled by the polymer–dye association constant.²¹

Polymer aggregation is a factor that influences the polymer quenching and consequently the performance of a polymeric biosensor, in various ways. The formation of aggregates reduces the fluorescence intensity of the polymer, and additionally, it may cause excitation energy transfer from the isolated polymer chains to aggregates, limiting the useful energy transfer from the polymer to the label dye. On the other hand, it was reported recently that the excitation energy transfer from a polymer to a dye (i.e., quenching of the polymer's fluorescence) is more efficient when the polymer is aggregated.^{21,22} Therefore, to optimize the performance of a polymeric biosensor, new WSCPs should be synthesized and the role of various parameters such as chemical structure, molecular conformation, molecular weight, and aggregation should be examined.

Motivated by this, in this paper, we study the effect of aggregation on the fluorescence decay dynamics of a recently synthesized cationic poly(fluorenevinylene-*co*-phenylenevinylene) (PFV-*co*-PV) in aqueous and EtOH solutions. The results were realized by means of femtosecond time resolved upconversion spectroscopy. A rapid excitation energy transfer from isolated to aggregated chains is observed in concentrated solutions. The contribution of the excitation energy transfer, of the isolated and aggregated chains on the overall fluorescence

* Corresponding author. E-mail: mfakis@physics.upatras.gr. Fax: +30 2610 997470.

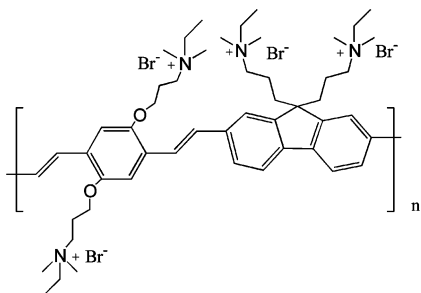


Figure 1. Chemical structure of the water-soluble PFV-co-PV.

decay of the polymer is determined. Finally, the dependence of the energy transfer parameters on the polymer concentration is also examined.

Experimental Section

The chemical structure of the polymer studied is shown in Figure 1. It was synthesized according to the following procedure:²³ Initially, a neutral poly(fluorenevinylene-co-phenylenevinylene) derivative with quaternizable tertiary amino groups was successfully synthesized by Heck coupling of 1,4-divinyl-3,6-(3'-bis(*N,N*-dimethylamino)propoxy)benzene with 2,7-dibromo-9,9-bis(3'-(*N,N*-dimethylamino)propyl)fluorene. This neutral polymer was treated with bromoethane to afford the quaternized cationic water-soluble PFV-co-PV polymer. The neutral polymer was soluble in common organic solvents, such as tetrahydrofuran, chloroform, and dichloromethane. The quaternized polymer did not dissolve in these solvents but was soluble in high polarity solvents, such as alcohols and water. The molecular weight, M_w , of the neutral polymer was determined by gel permeation chromatography using polystyrene as a standard and was found to be equal to 73 200 with a polydispersity equal to 1.57. Direct measurement of the cationic polymer's molecular weight was difficult because of the polymer aggregation on the column fillers induced by the ionic nature of the side chains.²⁴ However, since the quaternization reaction took place under mild conditions, the molecular weight and polydispersity of the cationic polymer are expected to be comparable to those of its neutral parent polymer. The quantum yield of the cationic polymer was found to be 0.14 using quinine sulfate as a standard.

Steady state fluorescence and PL excitation spectra were performed using a Perkin-Elmer LS55B luminescence spectrometer, while the absorption spectra were taken with a Beckman DU-640 spectrometer. The decay dynamics of the polymer were studied using femtosecond time resolved upconversion spectroscopy. The experimental setup has been described in detail previously.^{25,26} Briefly, the system consists of a mode-locked Ti:sapphire laser emitting 80 fs pulses at 800 nm with an 82 MHz repetition rate. The laser beam is frequency doubled into a BBO crystal (1 mm thickness), generating a second harmonic beam at 400 nm (6 mW average power). This beam excites the polymeric sample contained in a 1 mm thick quartz cuvette, while the remaining fundamental laser beam is used as the gate beam. The fluorescence of the sample is collected and focused together with the delayed gate beam onto a second BBO crystal (1.5 mm thickness), generating an upconversion beam. This upconversion beam is separated from the fundamental and fluorescence beams by an iris and filters and is directed into a monochromator. Finally, it is detected by a photomultiplier connected with a photon counter. The full width at half-maximum of the upconversion signal between the gate and the scattered from the sample excitation pulses gave the

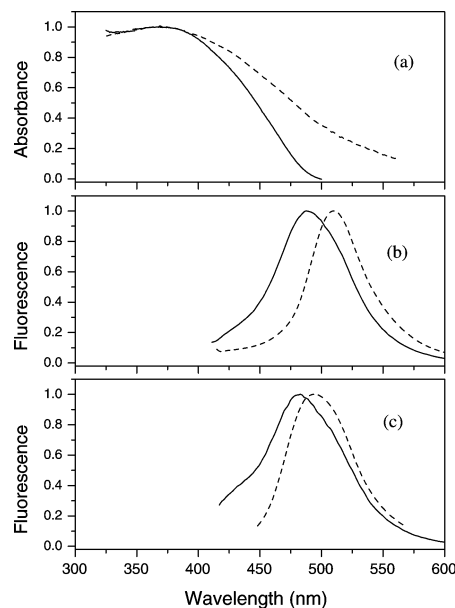


Figure 2. (a) Absorption and (b) fluorescence spectra of PFV-co-PV in dilute (solid line) and concentrated (dashed line) aqueous solutions. (c) Fluorescence spectra of PFV-co-PV in concentrated and dilute EtOH solutions.

temporal resolution of our system which was found to be equal to 250 fs. The spectral resolution of our system was 2.5 nm. The dynamics of the molecules was detected at different wavelengths across the emission spectrum under magic angle conditions.

Results and Discussion

Steady State Spectroscopy. Steady state spectroscopic measurements were performed on both dilute (10^{-4} wt %) and concentrated (10^{-1} wt %) polymer solutions. Figure 2a shows the absorption spectra of the PFV-co-PV in aqueous solutions. The absorption spectrum of a dilute solution is structureless with a peak at 380 nm. In a concentrated solution, the absorption spectrum has the same peak as the dilute one but exhibits a long tail extending to the red that is not present in the spectrum of the dilute solution. Similar spectra were obtained from EtOH solutions.

In Figure 2b, the fluorescence spectra of PFV-co-PV in water are shown. It is clear that the spectrum of the concentrated solution experiences a red shift compared to that of the dilute one. More specifically, the fluorescence peak shifts from 488 nm in the dilute solution to 510 nm in the concentrated solution. In Figure 2c, the fluorescence spectra of PFV-co-PV in EtOH, being slightly different from those in water, are shown. In dilute EtOH solution, a peak at 480 nm is observed, while, in concentrated solution, this is red-shifted to 500 nm. The fluorescence spectra in Figure 2b and c are shown in normalized intensity units so that the red shift is easily observed. However, the intensity of the concentrated solution spectra is significantly reduced (approximately 3 times) compared with that of the dilute ones, showing a lowering of the fluorescence quantum efficiency upon increasing the concentration.

The red shift of absorption and fluorescence spectra indicates the formation of aggregates in concentrated polymer solutions^{27–30} which has also been observed before in WSCPs.^{31,32} The driving force of aggregation is that the cationic polymer has a hydrophobic backbone and charged functional groups. In polar solvents, the polymer chains aggregate to minimize the exposure of the hydrophobic backbone on the polar environment.

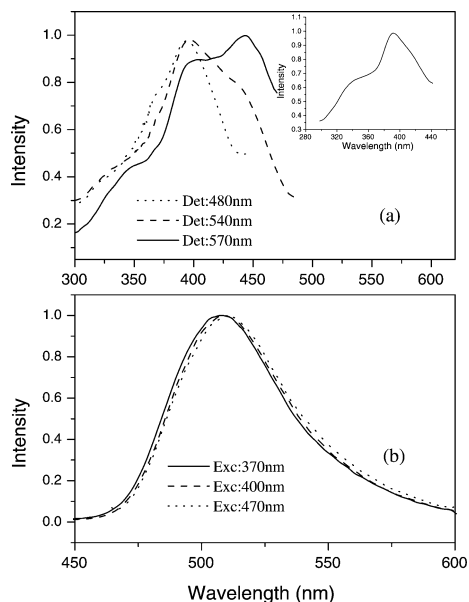


Figure 3. (a) Photoluminescence excitation spectra of PFV-co-PV (10^{-1} wt %) detected for three different emission wavelengths, 480, 540, and 570 nm. The inset shows the photoluminescence excitation spectrum of a dilute PFV-co-PV solution (10^{-4} wt %) for emission at 480 nm. (b) The fluorescence spectra of PFV-co-PV (10^{-1} wt %) detected for three different excitation wavelengths, 370, 400, and 470 nm.

Additional evidence for the aggregate formation in concentrated solutions is provided in Figure 3a where the PL excitation spectra of PFV-co-PV in a concentrated aqueous solution (10^{-1} wt %) are shown for three different detection wavelengths, namely, 480, 540, and 570 nm. By collecting the fluorescence at 480 nm (isolated chain emission band), the excitation spectrum exhibits a clear peak at 395 nm. As the detection wavelength shifts to the red (longer detection wavelength than 540 nm), a second peak appears at ~ 440 nm and its intensity becomes higher for the detection wavelength of 570 nm (aggregate emission band). This second peak in the PL excitation spectra is attributed to the excitation of aggregates. It is noted that, in dilute solutions, the excitation spectra show a single peak at 392 nm (inset of Figure 3a) and they are independent of the detection wavelength. Figure 3b shows the fluorescence spectra of PFV-co-PV in the same concentrated solution (10^{-1} wt %) detected for three different excitation wavelengths, namely, 370, 400, and 470 nm. The fluorescence spectra are almost independent of the excitation wavelength (maximum shift of only 2 nm). This indicates that even if the excitation wavelength lies in the isolated chain absorption band (370 nm), the isolated chain fluorescence (at wavelengths shorter than ~ 470 nm) is not observed because of self-absorption or energy transfer to aggregates, as will be discussed below.

Finally, it is noted that the spectrum of the PFV-co-PV polymer overlaps almost perfectly with the absorption spectrum of fluorescein which is commonly used as a label for DNA.^{15,33} Specifically, the absorption maximum of fluorescein is at ~ 495 nm³³ while as discussed before PFV-co-PV has a fluorescence maximum at 488 nm. Therefore, energy transfer from the PFV-co-PV to fluorescein could be favorable and PFV-co-PV can be an important candidate for DNA detection.

Time Resolved Spectroscopy. The fluorescence dynamics of PFV-co-PV has been studied at wavelengths across the fluorescence spectrum with a step of 10 nm. The excitation wavelength was 400 nm. In dilute solutions (10^{-4} wt %), the decay is nearly wavelength independent and monoexponential

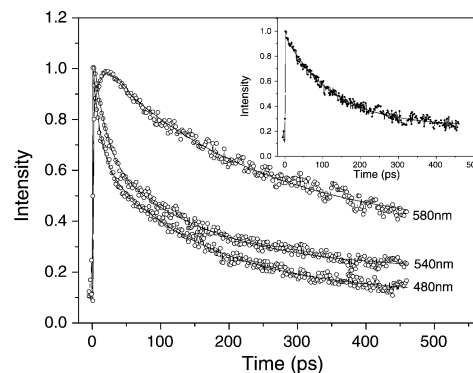


Figure 4. Fluorescence dynamics of PFV-co-PV at three characteristic wavelengths in aqueous solution of 10^{-1} wt % concentration together with the fits. The inset shows the fluorescence decay of PFV-co-PV in dilute aqueous solution.

TABLE 1: Pre-exponential Factors and Decay Time Constants Obtained from the Fits

λ_{em} (nm)	A_1	τ_1 (ps)	A_2	τ_2 (ps)	A_3	τ_3 (ps)
470	0.64	8 ± 1	0.36	135 ± 15		
480	0.62	8 ± 1	0.38	125 ± 12		
490	0.58	10 ± 2	0.42	120 ± 12		
500	0.5	14 ± 2	0.5	110 ± 10		
510	0.48	13 ± 3	0.52	130 ± 12		
520	0.47	13 ± 2	0.53	125 ± 11		
530	0.45	14 ± 3	0.55	110 ± 10		
540	0.36	13 ± 2	0.47	100 ± 12	0.17	290 ± 25
550	0.28	10 ± 2	0.44	110 ± 14	0.28	295 ± 30
560	0.17	11 ± 2	0.34	105 ± 14	0.49	320 ± 32
570	-0.2	8 ± 1			0.8	320 ± 32
580	-0.6	10 ± 2			0.9	340 ± 35

with a time constant of 120 ± 10 ps (inset of Figure 4). Using this value and the quantum yield, a radiative decay time of ~ 0.85 ns is calculated, typical of conjugated polymers. On the other hand, in concentrated solutions, the dynamics is wavelength dependent. The results for a concentrated aqueous solution (10^{-1} wt %) are shown in Figure 4 for three characteristic wavelengths. As can be seen, the fluorescence decays rapidly at short wavelengths while this decay becomes slower as the detection wavelength shifts to the red. The data were fitted to a sum of exponentials using the equation³⁴

$$I(t) = I_0 + \sum_i A_i \exp\left(-\frac{t}{\tau_i}\right) \quad (1)$$

where A_i and τ_i are the pre-exponential factors and the time constants of the different exponentials, respectively. I_0 is a parameter which represents the background noise of the detection system. Fitting the results, we distinguished three spectral regions where the decays were fitted using a different number of exponentials. Specifically, the decays at wavelengths ranging from 470 to 530 nm (short wavelength region) were fitted using two exponentials with decay times of approximately 8–14 and 100–140 ps, respectively. The decays at 540–560 nm (intermediate spectral region) were successfully fitted using three exponentials with decay times of 10–13, 100–110, and 290–320 ps, respectively. Finally, at 570 and 580 nm (long wavelength region), the decay was dominated by a slow rise followed by a single exponential with a long decay time of 320–340 ps. All parameters obtained from the fits are summarized in Table 1.

Similar qualitative behavior was shown from the dynamics of an EtOH solution of PFV-co-PV with a concentration of 10^{-1} wt %. The results are shown in Figure 5 at three characteristic

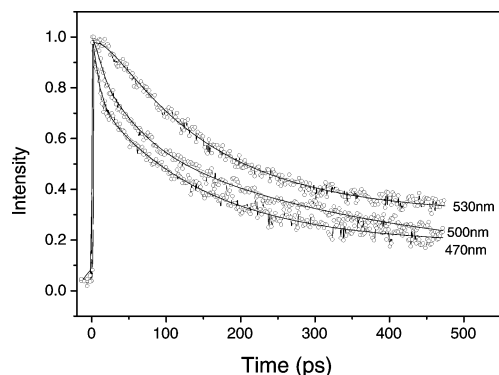


Figure 5. Fluorescence dynamics of the PFV-*co*-PV at three characteristic wavelengths in EtOH solution of 10^{-1} wt % concentration together with the fits.

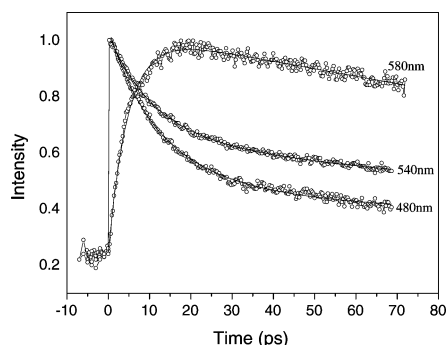


Figure 6. Fluorescence dynamics of PFV-*co*-PV in aqueous solution at 480, 540, and 580 nm within the first 70 ps.

emission wavelengths. Again, the dynamics at short wavelengths (470 and 500 nm) is governed by a rapid decay with a time constant of ~ 12 ps while the decay at long wavelengths is slower.

To obtain further insight on the dynamics of PFV-*co*-PV in aqueous solution, we focused on the rise of the fluorescence intensity at short and long wavelengths. The results are shown in Figure 6 for 480, 540, and 580 nm within the first 70 ps. A clear slow rise with a rise time of ~ 10 ps is observed in the dynamics at the long wavelength (580 nm). This slow rise of the fluorescence indicates that the species responsible for the emission at long wavelengths (aggregates) are mainly excited gradually during a time period much longer than the duration of the excitation pulse. Additionally, the rise time of the aggregate fluorescence is quite equal to the fast decay time (τ_1 in Table 1) of the fluorescence at short wavelengths (470–560 nm) where the isolated chains emit. Therefore, it is indicated that the aggregates are mainly excited through energy transfer from the energetically higher lying isolated chains.^{28,35–37} However, it is possible that a fraction of the aggregates may not participate in the energy transfer process and may be directly excited by their ground state.

We could now identify the origin of the different decay mechanisms at the three spectral regions in concentrated PFV-*co*-PV solutions. At the short wavelength spectral region (470–530 nm), it is suggested that the fast decay is due to energy transfer from isolated chains to aggregates. Afterward, the longer decay procedure at short wavelengths with a time constant of ~ 100 –140 ps is attributed to the normal fluorescence decay of isolated chains, since this decay time is similar to that observed in dilute solutions. At the intermediate spectral region (540–560 nm), the first two decay mechanisms (with decay times of ~ 10 and 100 –110 ps) are also attributed to the energy transfer and the isolated chain fluorescence, respectively. The third

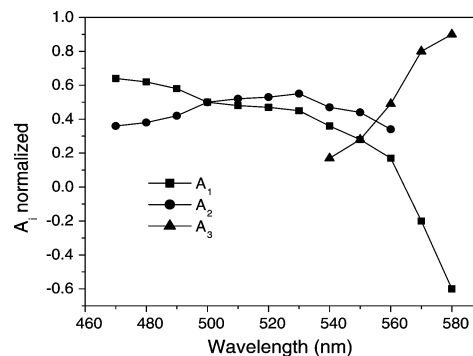


Figure 7. Normalized pre-exponential decay factors, A_i , as a function of the emission wavelength.

slower mechanism is attributed to emission from aggregates. Finally, at the long wavelength region apart from the slow rise of the fluorescence attributed to the excitation process of aggregates from isolated chains through energy transfer, the long monoexponential decay is attributed to aggregate emission. It should be mentioned, here, that since the polymer solutions under study are concentrated, one could consider the possibility of self-absorption and its effect on the dynamics. Self-absorption is actually a radiative energy transfer process where a photon is emitted by the donor molecule and is subsequently absorbed (before exiting the sample) by the acceptor molecule. Therefore, self-absorption does not compete with other decay mechanisms and the fluorescence decay time of the donor is unchanged.³⁸ For this reason, we believe that self-absorption is excluded from the interpretation of the dynamics.

On the basis of the analysis of the decay mechanisms as described before, the pre-exponential decay factors, A_i , in eq 1 now obtain a clear physical meaning. Thus, A_1 , A_2 , and A_3 represent the initial contributions ($t = 0$) of the energy transfer process, the isolated chain fluorescence, and the aggregated chain fluorescence, respectively, on the overall decay of the polymer. In Figure 7, these factors are shown in normalized units versus the emission wavelength. It is obvious that at short wavelengths (470–500 nm) the polymer fluorescence mainly decays through energy transfer from isolated to aggregate chains. At wavelengths from 510 to 550 nm, the dominant decay mechanism is the radiative deexcitation of isolated chains, while, at long wavelengths (560–580 nm), the overall decay is dominated by the emission of aggregates. It is noted that the energy transfer factor, A_1 , becomes negative at long wavelengths. This is due to the rise of the polymer's fluorescence, observed at these wavelengths, attributed to the energy transfer. The isolated chain factor, A_2 , does not appear in the long wavelength region, since at this region the isolated chain emission is very low (practically undetectable), as is shown in the dilute fluorescence spectrum (Figure 2b). Finally, the aggregate factor, A_3 , appears at wavelengths longer than 540 nm, meaning that aggregates do not emit at shorter wavelengths.

The effect of energy transfer on the polymer dynamics is also shown in the time resolved fluorescence spectra presented in Figure 8. In this figure, the fluorescence spectra at different times after excitation are depicted. During the first picoseconds, the short wavelength region dominates, showing that the emission mainly originates from isolated chains. However, due to the rapid energy transfer from isolated to aggregated chains and the subsequent slow decay of the aggregate emission, a gradual red shift of the emission spectra is observed. This red shift is clearly shown in the inset of Figure 8 where the emission spectra at 0.4 and 400 ps after excitation are shown in normalized units. It is seen that the aggregate emission band at

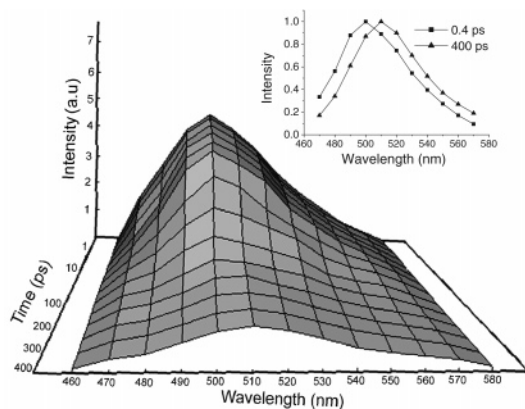


Figure 8. Fluorescence spectra of PFV-co-PV (10^{-1} wt %) detected at different times after excitation. The inset shows the spectra at 0.4 and 400 ps in normalized units.

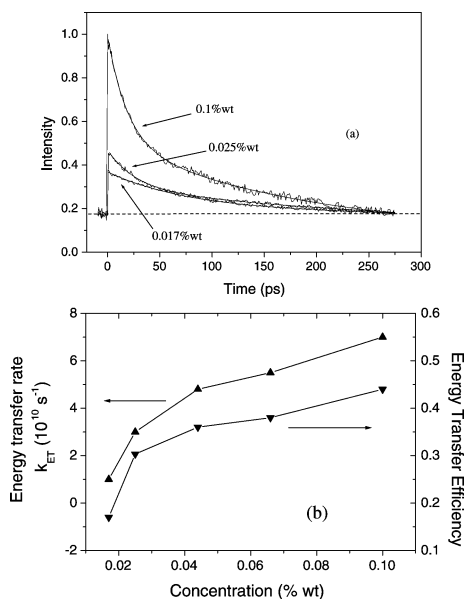


Figure 9. (a) Fluorescence dynamics of PFV-co-PV at 500 nm in aqueous solutions of different concentrations in absolute fluorescence intensity. (b) The energy transfer rate as well as the energy transfer efficiency as a function of concentration.

400 ps is enhanced in comparison to that at 0.4 ps at the expense of the isolated chain emission. It is noted that the fluorescence spectrum at 400 ps is identical to the corresponding steady state spectrum shown in Figure 2b.

For the investigation of the concentration effect on the dynamics and the energy transfer, solutions of different concentrations were studied. The results are shown in Figure 9a at 500 nm for three characteristic concentrations in absolute fluorescence units. It is seen that, as the concentration decreases, the decay becomes slower and the fast decay (indicating the energy transfer process) becomes less important. Specifically, for concentrations of 0.025 and 0.017 wt % (Figure 9a), the time constants of the fast decay are 33 and 70 ps, respectively, while, for 0.1 wt %, this is 14 ps. This is attributed to the limitation of the energy transfer in dilute solutions, since by diluting the solution the amount of aggregates decreases and the distance between isolated chains and aggregates increases.

The fact that the decay of the polymer's fluorescence becomes rapid when energy transfer occurs is an indication of a nonradiative Förster energy transfer.³⁸ Such a procedure results from short or long range interactions among molecules, and the distance between them is 10–100 Å. The energy transfer rate

can be calculated through the equation $k_{ET} = 1/\tau_1$, where τ_1 corresponds to the energy transfer time. For the concentrated polymer solution (10^{-1} wt %), k_{ET} is equal to $7 \times 10^{10} \text{ s}^{-1}$. Using the above equation, the energy transfer rate was calculated for different concentrations and the results are shown in Figure 9b. It is seen that k_{ET} decreases almost linearly as the concentration decreases while this decrease becomes more abrupt at concentrations lower than 0.04 wt %.

Finally, the energy transfer efficiency, Φ_{ET} , can be calculated using the measured decay times through the equation^{38,39}

$$\Phi_{ET} = 1 - \frac{\tau_D}{\tau_D^0} \quad (2)$$

where τ_D and τ_D^0 are the decay times in the presence and absence of acceptors—aggregates, respectively. In the presence of aggregates, however, the fluorescence decay is multiexponential, as discussed previously (Figures 4 and 5), and thus, τ_D is replaced by $\langle\tau_D\rangle$ which is the amplitude averaged decay time given by $\langle\tau_D\rangle = (\sum_i A_i \tau_i) / (\sum_i A_i)$ (I_0 is not taken into account, since this is a background noise factor which does not influence the dynamics). In the absence of acceptors, on the other hand, that is, where only isolated chains exist in the sample, the fluorescence decay of PFV-co-PV is a single exponential with a decay time equal to 120 ps. Using the data shown in Table 1 at 500 nm (concentration of 0.1 wt %), Φ_{ET} is found to be equal to 0.44. This means that 44% of the excited isolated chains transfer their excitation energy to aggregates. The dependence of Φ_{ET} on concentration follows almost the same dependence as k_{ET} , being 0.17 at 0.017 wt %, as shown in Figure 9b.

Conclusions

We have presented a novel cationic water-soluble conjugated copolymer emitting light at the blue-green spectral region, and we have studied its fluorescence dynamics in aqueous and EtOH solutions. The fluorescence dynamics in concentrated solutions were fitted with multiexponential functions, revealing an energy transfer process from isolated chains to aggregates. This energy transfer occurs within less than 14 ps and has an efficiency of 0.44 for a solution with a concentration of 0.1 wt %. The contribution of the energy transfer, the isolated chain fluorescence, and the aggregate emission on the overall decay of the polymer's fluorescence spectrum was determined. Finally, the dependence of the energy transfer parameters on concentration was examined. It was shown that, by reducing the concentration, the energy transfer efficiency and energy transfer rate decrease linearly, but this decrease becomes more abrupt at concentrations lower than 0.04 wt %.

Acknowledgment. We thank the European Social Fund (ESF), Operational Program for Educational and Vocational Training II (EPEAEK II), and particularly the Program PYTHAGORAS I, for funding the above work.

References and Notes

- (1) McGehee, M. D.; Heeger, A. J. *Adv. Mater.* **2000**, *12*, 1655.
- (2) Friend, R. H.; Gymer, R. W.; Holmes, A. B.; Burroughes, J. H.; Marks, R. N.; Taliani, C.; Bradley, D. D. C.; Dos Santos, D. A.; Brédas, J. L.; Lögdlund M.; Salanech, W. R. *Nature* **1999**, *397*, 121.
- (3) Sariciftci, N. S. *Curr. Opin. Solid State Mater. Sci.* **1999**, *4*, 373.
- (4) Sirringhaus, H.; Tessler, N.; Friend, R. H. *Science* **1998**, *10*, 365.
- (5) Shi, S. Q.; Wudl, F. *Macromolecules* **1990**, *23*, 2119.
- (6) McCormick, C. L. Water-soluble Polymers. In *Encyclopedia of Polymer Science and Engineering*; Kroschwitz, J. L., Ed.; Wiley-Interscience: New York, 1990.
- (7) Cabarcos, E. L.; Carter, S. A. *Macromolecules* **2005**, *38*, 4409.

- (8) Fan, Q.-L.; Zhou, Y.; Lu, X.-M.; Hou, X.-Y.; Huang, W. *Macromolecules* **2005**, *38*, 2927.
- (9) Wang, J.; Wang, D.; Miller, E. K.; Moses, D.; Bazan, G. C.; Heeger, A. J. *Macromolecules* **2000**, *33*, 5153.
- (10) Fan, Q.-L.; Lu, S.; Lai, Y.-H.; Hou, X.-Y.; Huang, W. *Macromolecules* **2003**, *36*, 6976.
- (11) Balanda, P. B.; Ramey, M. B.; Reynolds, J. R. *Macromolecules* **1999**, *32*, 3970.
- (12) Wagaman, M. W.; Grubbs, R. H. *Macromolecules* **1997**, *30*, 3978.
- (13) Liu, B.; Yu, W.-L.; Lai, Y.-H.; Huang, W. *Macromolecules* **2002**, *35*, 4975.
- (14) Chen, L.; McBranch, D. W.; Wang, H.; Helgeson, R.; Wudl, F.; Whitten, D. *Proc. Natl. Acad. Sci. U.S.A.* **1999**, *96*, 12287.
- (15) Gaylord, B. S.; Heeger, A. J.; Bazan, G. C. *Proc. Natl. Acad. Sci. U.S.A.* **2002**, *99*, 10954.
- (16) Gaab, K. M.; Bardeen, C. J. *J. Phys. Chem. B* **2004**, *108*, 4619.
- (17) Ruseckas, A.; Theander, M.; Valkunas, L.; Andrsson, M. R.; Inganas, O.; Sundström, V. *J. Lumin.* **1998**, *76* and *77*, 474.
- (18) Grage, M.; Zaushtsym, Y.; Yartsev, A.; Chachisvillis, M.; Sundström, V.; Pullerits, T. *Phys. Rev. B* **2003**, *67*, 205207.
- (19) Peng, K.-Y.; Chen, S. -An.; Fann, W.-S. *J. Am. Chem. Soc.* **2001**, *123*, 11388.
- (20) Förster, T. *Ann. Phys.* **1948**, *2*, 55.
- (21) Tan, C.; Atas, E.; Müller, G. G.; Pinto, M. R.; Kleiman, V. D.; Schanze, K. S. *J. Am. Chem. Soc.* **2004**, *126*, 13685.
- (22) Tan, C.; Pinto, M. R.; Schanze, K. S. *Chem. Commun.* **2002**, 446–447.
- (23) Mikroyannidis, J. Unpublished data.
- (24) Huang, F.; Wu, H.; Wang, D.; Yang, W.; Cao, Y. *Chem. Mater.* **2004**, *16*, 708.
- (25) Anastopoulos, D.; Fakis, M.; Polyzos, I.; Tsigaridas, G.; Persephonis, P.; Giannetas, V. *J. Phys. Chem. B* **2005**, *109*, 9476.
- (26) Fakis, M.; Polyzos, I.; Tsigaridas, G.; Giannetas, V.; Persephonis, P. *Chem. Phys. Lett.* **2004**, *394*, 372.
- (27) Fakis, M.; Polyzos, I.; Tsigaridas, G.; Giannetas, V.; Persephonis, P.; Spiliopoulos, I.; Mikroyannidis, J. *Phys. Rev. B* **2002**, *65*, 195.
- (28) Blatchford, J. W.; Jessen, S. W.; Lin, L. B.; Gustafson, T. L.; Fu, D. K.; Wang, H. L.; Swager, T. M.; MacDiarmid, A. G.; Epstein, A. J. *Phys. Rev. B* **1996**, *54*, 9180.
- (29) Nguyen, T.-Q.; Doan, V.; Schwartz, B. J. *J. Chem. Phys.* **1999**, *110*, 4068.
- (30) Collison, C. J.; Rothberg, L. J.; Treemanekarn, V.; Li, Y. *Macromolecules* **2001**, *34*, 2346.
- (31) Wang, D.; Lal, J.; Moses, D.; Bazan, G. C.; Heeger, A. J. *Chem. Phys. Lett.* **2001**, *348*, 411.
- (32) Hua, F.; Ruckenstein, E. *Langmuir* **2004**, *20*, 3954.
- (33) Xu, Q.-H.; Gaylord, B. S.; Wang, S.; Bazan, G. C.; Moses, D.; Heeger, A. J. *Proc. Natl. Acad. Sci. U.S.A.* **2004**, *101*, 11634.
- (34) McCutcheon, M. W.; Young, J. F.; Pattantyus-Abraham, A. G.; Wolf, M. O. *J. Appl. Phys.* **2001**, *89*, 4376.
- (35) Herz, L. M.; Silva, C.; Phillips, R. T.; Setayesh, S.; Mullen, K. *Chem. Phys. Lett.* **2001**, *347*, 318.
- (36) Palsson, L.-O.; Wang, C.; Russel, D. L.; Monkman, A. P.; Bryce, M. R.; Rumbles, G.; Samuel, I. D. W. *Chem. Phys.* **2002**, *279*, 229.
- (37) Mahrt, R. F.; Pauck, T.; Lemmer, U.; Siegner, U.; Hopmeier, M.; Hennig, R.; Bassler, H.; Gobel, E. O.; Bolivar, P. H.; Wegmann, G.; Kurz, H.; Scherf, U.; Mullen, K. *Phys. Rev. B* **1996**, *54*, 1759.
- (38) Valeur, B. *Molecular Fluorescence: Principles and Applications*; Wiley-VCH Verlag: New York, 2001.
- (39) Varnaski, O.; Samuel, I. D. W.; Palsson, L.-O.; Beavington, R.; Burn, P. L.; Goodson, T., III. *J. Chem. Phys.* **2002**, *116*, 8893.